Biosensors and Bioelectronics 137 (2019) 287–293

Contents lists available at ScienceDirect

Biosensors and Bioelectronics

journal homepage: www.elsevier.com/locate/bios

Development of a methodology for reversible chemical modification of silicon surfaces with application in nanomechanical biosensors

Roseli H. Sato[a], Priscila M. Kosaka[b], Álvaro T. Omori[a], Edgard A. Ferreira[c], Denise F.S. Petri[d], Óscar Malvar[b], Carmen M. Domínguez[b], Valerio Pini[b], Óscar Ahumada[e], Javier Tamayo[b], Montserrat Calleja[b], Rodrigo L.O.R. Cunha[a], Pablo A. Fiorito[f,*]

[a] CCNH, Centro de Ciências Naturais e Humanas, Universidade Federal do ABC, UFABC, Avenida dos Estados, 5001, 09210-580, Santo André, São Paulo, Brazil
[b] Instituto Micro y Nanotecnología (IMN-CNM), CSIC, Isaac Newton 8 (PTM), Tres Cantos, Madrid, Spain
[c] Escola de Engenharia, Universidade Presbiteriana Mackenzie, 01302-907, São Paulo, SP, Brazil
[d] Departamento de Química Fundamental, Instituto de Química, Universidade de São Paulo, P.O. Box 26077, São Paulo, SP, 05513-970, Brazil
[e] Mecwins S.A, Plaza de la Encina 10-11, Núcleo 5, 2 B, 28760, Tres Cantos, Madrid, Spain
[f] Centro de Investigaciones y Transferencia Villa María (CIT VM - CONICET), Instituto de Ciencias Básicas y Aplicadas, Universidad Nacional de Villa María, Av. Arturo Jauretche 1555, Villa María, C.P, 5900, Córdoba, Argentina

ARTICLE INFO

Keywords:
Biosensor
Microcantilever
Chalcogen chemistry
Surface regeneration
Nanomechanical biosensors
Reversible immobilization

ABSTRACT

Hypervalent tellurium compounds have a particular reactivity towards thiol compounds which are related to their biological properties. In this work, this property was assembled to tellurium-functionalized surfaces. These compounds were used as linkers in the immobilization process of thiolated biomolecules (such as DNA) on microcantilever surfaces. The telluride derivatives acted as reversible binding agents due to their redox properties, providing the regeneration of microcantilever surfaces and allowing their reuse for further biomolecules immobilizations, recycling the functional surface. Initially, we started from the synthesis of 4-((3-((4-methoxyphenyl) tellanyl) phenyl) amino)-4-oxobutanoic acid, a new compound, which was immobilized on a silicon surface. In nanomechanical systems, the detection involved a hybridization study of thiolated DNA sequences. Fluorescence microscopy technique was used to confirm the immobilization and removal of the telluride-DNA system and provided revealing results about the potentiality of applying redox properties to chalcogen derivatives at surfaces.

1. Introduction

Biosensors are analytical devices that use a biological recognition layer attached to a solid transducer that converts a physicochemical event caused by a biological response into a measurable signal. They must be highly specific, robust and sensitive, and should be reusable. Biosensors have extensive use in various fields such as drug discovery, biomedicine, diagnosis, food safety, environmental monitoring, security, and defense. The biosensors business involves approximately 10 billion dollars annually, becoming an attractive field of interdisciplinary research because of a potential revolution in the development of new diagnoses tests, healthcare and consumer (Goode et al., 2015).

In the last decade, nanotechnology has provided a wide variety of nanobiosensors with a potential to replace traditional testing procedures that require specific expertise and time, representing a considerable cost in their specific fields. Some representative examples include electrical biosensors based on semiconductor nanowires (Ahmad et al., 2018), optical biosensors based on metallic nanoparticles (Malekzad et al., 2018; Viter et al., 2017), and nanomechanical biosensors such as micro- and nanocantilevers (Kartanas et al., 2017; Zhou et al., 2018). Optical and electrical transductions still dominate the research in biosensors, but the field of nanomechanical biosensors is growing and will play an essential role during the next years. Nanomechanical biosensors are usually cantilever-shaped and are fabricated using well-established semiconductor technology that enables the batch production of arrays with hundreds of nanomechanical systems. Nanomechanical systems can exhibit extremely low mechanical compliances translating biomolecular recognition events into measurable displacements and vibrational properties of the nanomechanical structures when adsorption of biomolecules or biomolecular interactions take place on the nanomechanical system surface (Arlett et al., 2011;

* Corresponding author.
E-mail address: fiorito@unvm.edu.ar (P.A. Fiorito).

https://doi.org/10.1016/j.bios.2019.04.028
Received 26 January 2019; Received in revised form 9 April 2019; Accepted 14 April 2019
Available online 27 April 2019
0956-5663/ © 2019 Elsevier B.V. All rights reserved.

Bañuls et al., 2010; Boisen et al., 2011; Buchapudi et al., 2011; Calleja et al., 2012; Consortium, 2012; Eom et al., 2011; Lan et al., 2005). Microcantilever sensors have been used for a wide range of applications such as the detection of cancer cells (Etayash et al., 2015; Chen et al., 2016; Pandya et al., 2015), proteins (Wu et al., 2001; Lee et al., 2005; Arntz et al., 2003; Kosaka et al, 2013, 2014, 2017; Agarwal et al., 2018), DNA (Calleja et al., 2005; Biswal et al., 2006; Mertens et al., 2008; Domínguez et al., 2015) mRNA (Duffy et al., 2018), bacteria (Longo et al., 2013; Wang et al., 2014; Kasas et al., 2015; Malvar et al., 2016) and humidity (Del Rey et al., 2014). However, just like most nanotechnologies, nanomechanical sensors have not been translated into valid clinical tests because there are some pitfalls and issues regarding specificity, reproducibility, reliability and high costs that must be solved. Although many strategies are being pursued to bring down the costs of these biosensors, cheaper electronics components and circuits have contributed to reduce the costs as well as to develop low-cost disposable transducers. For some applications, however, high-grade transducers are required and sensor surface regeneration may be a key technique in lowering costs per test. Currently, tests costs are an obstacle for the use of biosensors that address the needs of developing countries such as food safety, water sanitation, healthcare, and diagnostic tools during diseases outbreaks, unfortunately. Therefore, there is an increasing interest in the development of strategies for introducing the regeneration of sensor surfaces for the development of biosensors that can be used more than once (Li et al., 2018; Zhou et al., 2018; Knoglinger et al., 2018; Duan et al., 2013; Loo et al., 2011).

Organotellurium compounds (Nogueira et al., 2004; Cunha et al., 2009a) have shown interesting properties such as enzyme inhibition cathepsins (Cunha et al., 2005, 2009b; Caracelli et al., 2012), antiparasitic activities (Pimentel et al., 2012; Maluf et al., 2016), antimicrobial activity (Daniel-Hoffmann et al., 2012), and growth and apoptosis in certain cancer cells lineages (Engman et al., 2000; Abondanza et al., 2008; Silberman et al., 2016) and anticonvulsant activities (Persike et al., 2008). In 1994, Detty and Engman groups independently demonstrated the redox activity (Detty et al., 1994; Engman et al., 1994) of organotellurides to convert catalytically thiols into disulfides. This work seminally established the application of organotellurides as thiol-peroxidase mimetics (for a recent example: Tanini et al., 2018). Besides these developments from last decades, the attachment organotellurium moieties on surfaces can point out novel properties to functional materials that have not been previously thought of. The plethora of preparation methods of organic tellurides, the facile tellurium oxidation to hypervalent states, its rapid reactions with thiols and the detachment of the thiolated species by reduction of Te-S bond may lead to the desired property of reusable surfaces for biosensing, providing a flexible and cost-effective alternative for the surface regeneration of biosensor surfaces. In this work, we propose a new application of these compounds beyond organic synthesis and biological studies, using a bisaryl telluride to anchor at a silicon surface through an amide bond and check the reversible chemical modification on silicon surfaces for the label-free detection of DNA using nanomechanical sensors.

2. Materials and methods

2.1. Organotelluride synthesis

The synthesis of the designed organotelluride (**3**) is described in Supporting Information. Briefly, it comprises a modification of a previous work and was based on the procedure presented by Clark (Clark et al., 2002).

2.2. Surface modification

The designed organotelluride-functionalized succinamic acid (compound **3**) was immobilized on the surface of silicon wafers (single-side polished, ⟨100⟩, N-type, no dopant) purchased from Sigma-Aldrich, with an area of 0.25 cm^2 and 0.5 mm of thickness. These wafers were washed three times in toluene (Sigma-Aldrich), methanol (Sigma-Aldrich), Milli-Q water and then dried under nitrogen flux. The surface was activated with piranha solution (caution: piranha solution is extremely corrosive, reactive and potentially explosive), sulfuric acid (Sigma-Aldrich) and hydrogen peroxide (Sigma-Aldrich) (3 : 1) for 20 min and washed with Milli-Q water. The silicon surfaces were functionalized with a solution of (3-aminopropyl) triethoxysilane 98% (Sigma-Aldrich) 4×10^{-3} mol L^{-1} in anhydrous toluene (Sigma-Aldrich) for 2 h and washed with toluene and dried with N_2. For the coupling of telluride acid, a solution of telluride 4 x 10^{-3} mol L^{-1}, *N*-(3-dimethylaminopropyl)-*N′*-ethylcarbodiimide hydrochloride (Sigma-Aldrich) 8×10^{-2} mol L^{-1} and *N*-hydroxysuccinimide (Sigma-Aldrich) 12×10^{-2} mol L^{-1} was prepared in anhydrous methanol (Sigma-Aldrich) in an overnight reaction. The wafers were washed with methanol and dried under nitrogen flux. After the immobilization, the telluride was oxidized with hydrogen peroxide to form telluroxide, the species that would link to the thiol group present on the structure of the biomolecule, for 20 min and dried under nitrogen flux.

The following synthetic thiolated DNA sequences purchased from Stab Vida (Caparica, Portugal) were used for the immobilization on the sensor surface, detection of DNA and negative control samples:

- SH-DNA (probe): 5′-GCCGACTGTCGGCGCTGGG-3′-C_3H_6-SH
- C-DNA (complementary probe): 5′-GTGTTAGCTTGTGGTGGTC-3′
- Poly AC-SH (negative control): 5′ ACA CAC ACA CAC ACA CAC A-3′
- T5 DNA-SH-CY3 (fluorescence microscopy) 5′ CAA TGC AGA TAC ACT TTT TT-3′

In the procedure of DNA immobilization, aliquots of SH-DNA (6 μmol L^{-1}) were prepared in Te-NaCl buffer 1 mol L^{-1} (Sigma-Aldrich). A solution of 6 μmol L^{-1} thiolated ssDNA (SH-DNA) was prepared in Te-NaCl degassed buffer (to avoid the formation of disulfides), the microcantilever arrays were incubated overnight at room temperature (RT) and under agitation (rotation of 400 rpm). After this, the samples were washed twice with the following buffers: PBS (Sigma-Aldrich)/NaCl (Sigma-Aldrich)/$MgCl_2$ (Sigma-Aldrich) at pH = 7.5 for 5 min and room temperature and PBS at pH = 7.5 for 20 min and room temperature. The samples were then washed with Milli-Q water and dried under nitrogen flux.

The samples were in contact with BSA solution (1 mg mL^{-1}) prepared in Milli-Q water for 1 h, at room temperature and under agitation (rotation of 400 rpm); this procedure enabled surface coverage with BSA molecules avoiding unspecific interactions. After that, the wafers were washed three times with Milli-Q water and dried in a nitrogen flux.

For the DNA detection, the dsDNA was subjected to a similar procedure of DNA immobilization, which differed in the degassing step (which is not necessary for this sequence because of the absence of thiol groups) and incubated overnight at 30 °C.

The process of immobilization and hybridization of the DNA control, Poly AC-SH, followed the methodology described in the procedure of the SH-DNA and C-DNA sequences.

Before the step of reduction, samples were cleaned with Triton X-100 (Sigma-Aldrich) 1% in MilliQ water for 2 h under agitation (700 rpm) at room temperature. The microcantilevers were washed three times with Milli-Q water and dried in a nitrogen flux.

In the step of reduction, a solution of 1, 4-dithiothreitol (Sigma-Aldrich) in methanol 20×10^{-3} mol L^{-1} was used for 3 h with a rotation of 700 rpm. After this period, the samples were washed three times with methanol and dried under nitrogen flux.

The procedures of immobilization, drying and cleaning of the microcantilevers were developed in eppendorf tubes; the chips were held with small teflon clamps to prevent them from hitting the walls of the tubes, thus avoiding their breakage.

2.3. Contact angle measurements

The contact angle measurements were performed in a home-built apparatus, equipped with a digital camera (Nikon D40-X) connected to a computer. The volume used in this study was 10 μL of Milli-Q water. After each step of surface modification, the values of the angle (n = 5) were obtained, and the data were processed with Image J software (https://imagej.nih.gov/ij/).

2.4. Ellipsometric measurements

Ellipsometric measurements were performed in air using a vertical computer-controlled DRE EL02 ellipsometer (Ratzeburg, Germany). The angle of incidence was set at 70.0°, and the wavelength, λ, of the He-Ne laser was 632.8 nm. For data interpretation, a multilayer model composed of the substrate, the unknown layer, and the surrounding medium was used. Then, the thickness (d_x) and refractive index (n_x) of the unknown layer can be calculated from the ellipsometric angles, Δ and ψ, using the fundamental ellipsometric equation and iterative calculations with Jones matrices (Azzam and Bashara, 1987)

$$e^{i\Delta} \tan \Psi = \frac{R_p}{R_s} = f(n_x, d_x, \lambda, \phi)$$

where Rp and Rs are the overall reflection coefficients for the parallel and perpendicular waves. These coefficients are a function of the angle of incidence φ, the wavelength λ of the radiation, and the refractive index and thickness of each layer of the model.

From the ellipsometric angles Δ and Ψ and a multilayer model it is possible to determine the thickness of each deposited layer on Si wafers, namely, APTES, telluride compound immobilization, DNA immobilization and recognition, surface blocking with BSA, and surface recovering, First of all, the thickness of the SiO_2 layers was determined in air, considering the refractive index for Si as $\tilde{n} = 3.88 - i0.018$ (Edward, 1985) and its thickness as an infinite one, for the surrounding medium (air) the refractive index was considered as 1.00. Because the native SiO_2 layer is very thin, its refractive index was set as 1.462 (Edward, 1985) and just the thickness was calculated. The mean thickness and the corresponding standard deviation determined for each layer were native SiO_2 layer (1.96 ± 0.08) nm, APTES (1.55 ± 0.14) nm, Te (0.80 ± 0.24) nm, DNA-SH (0.30 ± 0.16) nm and DTT (0.84 ± 0.07) nm.

2.5. Nanomechanical measurements

The surface stress was measured using the scanning laser beam SCALA® (Mecwins, Spain) in controlled conditions: temperature of 24 °C and equilibrated at 0% relative humidity under a flow of dry nitrogen for 1 h. The silicon microcantilevers used, 500 μm in length, 100 μm in width and 1 μm in thickness, were purchased from Concentris (Basel, Switzerland).

The experiments were performed in a SCALA-Bio platform (MecWins, Spain) where readout was made directly from a 96-well plate coated with polydimethylsiloxane (PDMS) to attach the microcantilever chips to its surface. The read-out of the microcantilever deflections is based in the automated two-dimensional scanning of a laser beam across the surface of each microcantilever, and the collection of the reflected beam on the surface of a two-dimensional position sensing linear detector (PSD) orthogonally oriented to the reflected beam. The system was equipped with an environmental chamber with capability to keep temperature at 25.00 ± 0.02 °C and to change relative humidity at a rate of 10.00 ± 0.08% min^{-1}.

The measurements were performed before and after incubation with the problem solution.

Table 1
Mean values and corresponding standard deviations of contact angle (CA) measurements determined for five samples after each step of surface modification.

Surface modification	CA (°)
Oxidation (piranha solution)	36 ± 4
Silanization (APTES)	77 ± 2
Telluride immobilization	73 ± 3
Telluride oxidation	64 ± 3
DNA immobilization	38 ± 3
Blocking (BSA)	63 ± 1
Complementary strand (detection process)	39 ± 2
Reduction of telluride (surface regeneration)	68 ± 3

3. Results and discussion

3.1. Surface analysis (contact angle and ellipsometry)

Contact angle measurements were used as a first approach to optimize the methodology developed for the reversible chemical modification of silicon surfaces with telluride immobilized. In this study, all steps involved in the surface modification, starting from surface activation to the final step of the reduction procedure, were monitored by means of contact angle measurements, as presented in Table 1.

The analysis of the data obtained from the contact angle (Table 1) allowed to verify the redox properties of telluride immobilized on the silicon surface. The contact angle after the reduction process (68 ± 3) was very close to the initial value of telluride before oxidation (73 ± 3). Changes of the contact angle values for water on the modified surface were perceptible on the steps of immobilization of telluride, immobilization of the DNA sequence and reduction of telluride. This effect is related to the formation of hydrophobic and hydrophilic groups on the surface. The immobilization of telluride on the surface provided hydrophobic characteristics because of the presence of aromatic groups. In order to immobilize a SH-DNA sequence, the telluroxide would form a link between telluride and the thiol group present in the modified DNA sequence. Therefore, before the immobilization process, the telluride was oxidized with hydrogen peroxide to form telluroxide, but in the presence of water, this species is converted to dihydroxy telluride, which is responsible for the formation of the Te-S binding (Kanda et al., 1999; You et al., 2003) This process (with change of angle value from 73° ± 3–64° ± 3) might indicate the presence of dihydroxy telluride (hydrophilic) on the surface. After that, the SH-DNA sequence was immobilized and the contact angle value was of 38° ± 3, the sugar-phosphate backbone present in the DNA structure is hydrophilic and allows the DNA backbone to form bonds with water. The surface was blocked using bovine serum albumin BSA to avoid unspecified interactions of molecules with the surface, and the angle value changed from 38° ± 3–63° ± 1. In the hybridization process, it was possible to identify the angle variation from 63° ± 1–39° ± 2, which might be related to the presence of hydrophilic groups in the DNA chain. The process of reduction of chalcogen was accomplished using a reducing agent (DTT), which changed the angle value from 39° ± 2–68° ± 3, approaching the value of telluride before immobilization of DNA.

The mean values of film thicknesses relative to each step of surface modification were determined by ellipsometry, which is a complementary technique for contact angle measurements. With he techniques of surface analysis was possible to monitor the surface reversibility because of redox properties of Te compounds, allowing a new modification procedure. Fig. 1 shows the results obtained in techniques of surface analysis, where it can be seen the changes in the contact angle after every modification step (above figure) and a scheme showing the mechanism proposed for the cantilever modification process (figure below) of this work.

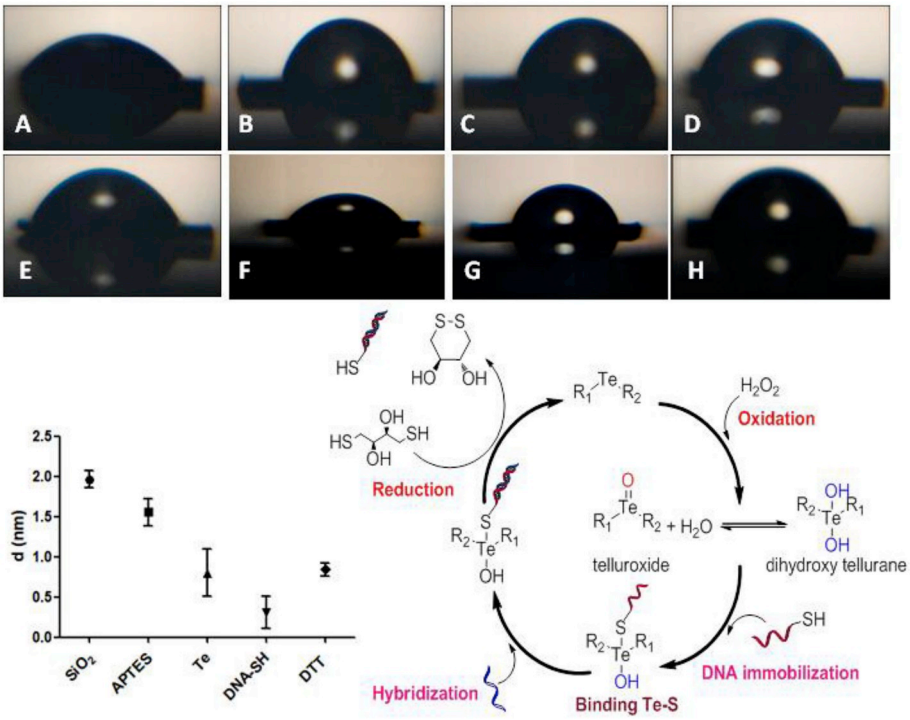

Fig. 1. Surface analysis: A-oxidation with piranha solution, B- APTES self-assembled monolayer, C-telluride (3a) immobilization, D-oxidation of telluride, E- DNA immobilization, F- surface blocking (BSA), G-complementary strand (ds-DNA) and H-reduction of telluride (surface regeneration). The graph illustrates the layer thickness variation of each process by ellipsometry: SiO_2 (1.960 ± 0.08485 nm), APTES (1.554 ± 0.1389 nm), Te (0.7980 ± 0.2376 nm), DNA-SH (0.3040 ± 0.1624 nm) and DTT (0.8420 ± 0.06686 nm) (one-way ANOVA: Tukey Test).

The results obtained with ellipsometry are shown as inset in Fig. 1, and allow to verify that the thickness of telluride, before and after the reduction process, was similar, showing total agreement with the results obtained with the contact angle technique. The Scheme in Fig. 1 shows the proposed mechanism for modifying silicon surfaces via telluride immobilization, and the importance of telluride oxidation to form the Te-S binding, responsible for the immobilization of molecular recognition elements. After the detection of target molecules, the reduction process regenerates the surface, allowing to perform a new immobilization cycle.

3.2. Nanomechanical measurement

The surface modification methodology developed using contact angle measurements was applied to nanomechanical biosensors for the detection of DNA hybridization. In this way, we could demonstrate the reversible nature of the chemical bond between the thiolated biomolecule probe and the telluride compound and thus determine how many times a sensitive and specific detection of the complementary DNA sequence was achieved using microcantilevers with the regenerated surfaces. Scheme 1 presents the process developed in microcantilevers.

It is very important to point out that the immobilization of thiolated biomolecules on silicon surfaces eliminated the need of gold-coating in one of the surfaces of the microcantilever, the presence on a gold-coated surface can be a source of non-specific cantilever bending due to variations in temperature (Ramos et al., 2007). Therefore, due to the insensitivity of our microcantilever device to temperature changes, the equipment costs decreased tremendously as we did not need specialized equipment for accurate temperature control.

Since the process of detection was performed on static mode, telluride was oxidized only on the top microcantilever surface. In order to ensure that the microcantilever is oxidized only in its upper part, it is placed inverted over the hydrogen peroxide solution during the oxidation step; the lower density of the cantilever and the surface tension of the liquid allow the material to float, ensuring that the chemical modification occurs only on one side of the cantilever (Kosaka et al., 2013). This methodology guaranteed the asymmetric immobilization needed, and thus the variation of surface energy from elastic contraction or expansion in relation to the opposite surface could be measured.

Fig. 2 shows the variation of the surface stress acquired in each use of the microcantilever.

The analysis of surface stress performance, displayed in Fig. 2A, allowed to verify that the sensitive and specific detection of DNA hybridization was possible in the first and second use, indicating that the redox property of the telluride immobilized on the microcantilever surface was maintained. In the third use of the microcantilever there was no change in the surface stress values and thus none detection of the DNA sequence. The decrease in the detection response may be related to the capacity of the telluride reduction due to steric problems. This effect is related to the conformation of the DNA anchored on the telluride layer. If the DNA sequence acquires tangle conformation during the hybridization process, the reduction reaction might be affected as the reducing agent was not able to reach the binding site between the chalcogen and the thiol present on the surface.

Another system analyzed was the negative control samples to verify whether the signal obtained by the detection system was specifically due to the recognition of the complementary DNA probe. Fig. 2 (B) shows that the change in the surface stress measured for the microcantilevers functionalized with the negative control probe was negligible. The specificity was maintained on the second and third reuse of the microcantilevers functionalized with the control probe.

After verifying the applicability of telluride in the immobilization and hybridization processes of DNA, the next study was the immobilization of different sequences in the same microcantilever: First, the Poly AC-SH (negative control) sequence was immobilized and the detection/reconstitution sequence was carried out. Next, two SH-DNA immobilization cycles were performed. The results obtained are presented in Fig. 2C, where it can be observed that the SH-DNA/C-DNA recognition process was successful in the second cycle. This proves that it was possible to immobilize different DNA sequences without interference on the detection on the second use of the sensor. The first sequence immobilized was the negative control, and the changes in surface stress values were negligible. After the reduction process, the second and third DNA sequence immobilized was SH-DNA (detection sample), and the surface stress values observed indicated that the

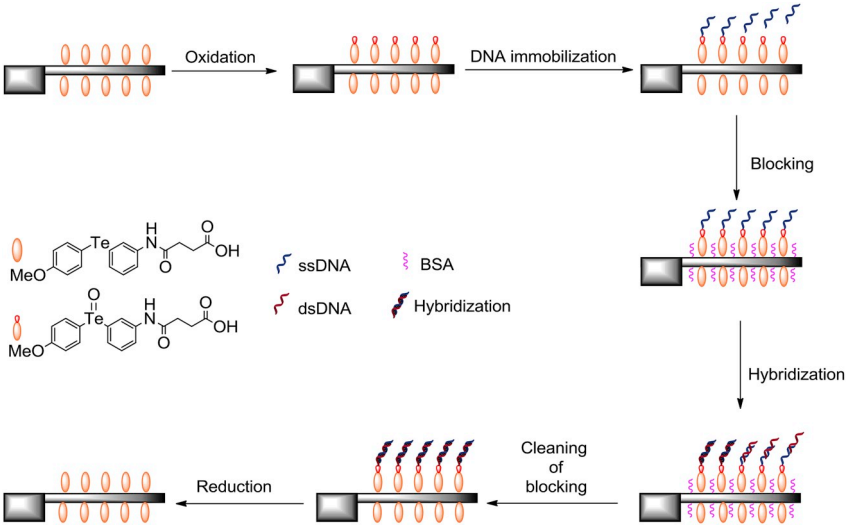

Scheme 1. Schematic representation of the immobilization process using telluride and DNA sequences. In this system, telluroxide was formed only on the active surface of the microcantilever to ensure the detection response.

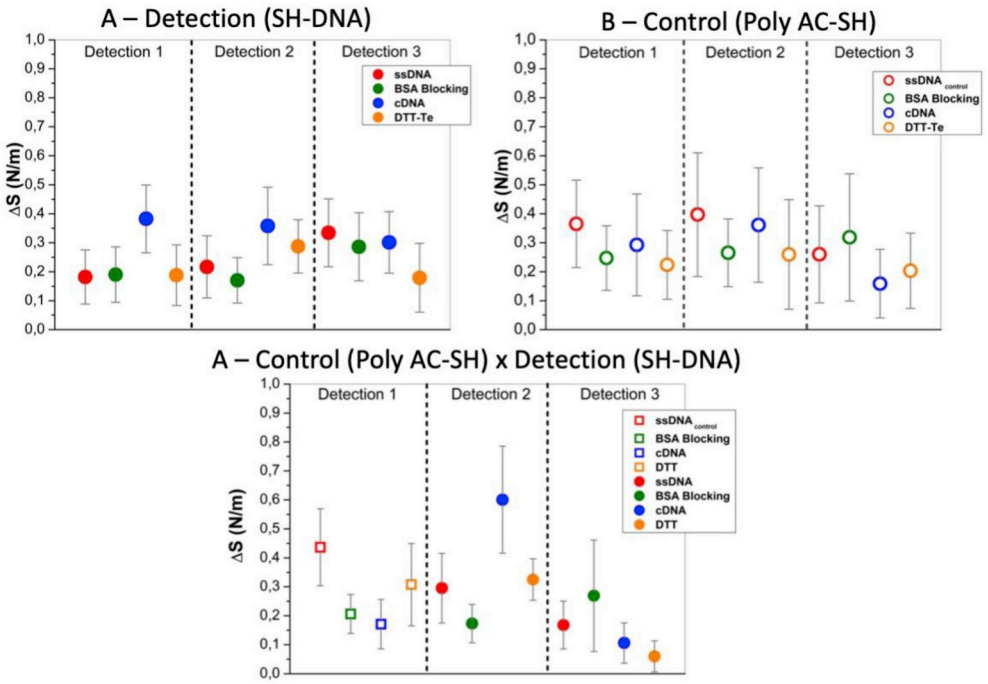

Fig. 2. Variation of surface stress values on three immobilization-detection cycles, on static mode, of (A) C-DNA (detection sample), (B) Poly AC-SH (control sample) and (C) change of sequences: first immobilization of DNA negative control (Poly AC-SH) and second and third of DNA detection probe (C-DNA). Three detection cycles were performed in the three systems.

hybridization with the complementary sequence occurred on the second recognition step; again, in the third measurement the response of hybridization was not as effective as the in second microcantilever use.

Comparison between the two systems (detection and control) allowed to verify that the process to remove the thiolated biomolecule was effective. This suggests that the use of telluride compounds can be a promising and cheaper alternative to gold for immobilization of thiolated probes in biosensing applications.

In Fig. 3 can be observed the comparative analysis between the detection and control systems, and the statistical analysis between the samples and the numbers of measurements.

A total of 96 microcantilevers were used: 64 microcantilevers were used for the detection of C-DNA sequence; 16 microcantilevers were used as negative control (Poly AC-SH sequence immobilized onto the microcantilever surface) to check the specificity of the biosensor; 16 microcantilevers that were first immobilized with the Poly AC-SH negative control sequence and then (after the removal of the negative control sequence from the microcantilever surface) functionalized with the SH-DNA probe for the C-DNA sequence detection. Each microcantilever array was reused for 3 times, that is, the immobilization and removal processes of the thiolated DNA sequence (detection or control) were performed three times in each microcantilever.

The comparative analysis between control and detection samples provided critical information about telluride: the presence of this compound on the surface of microcantilever did not interfere in the hybridization response. This information is crucial because it shows the applicability of telluride derivatives as a tool for application on surface functionalization using the reversibility of thiol binding according to the oxidation state of the tellurium atom. The analysis allowed to verify that, in the third detection step, the response in these two systems presented a rate of false positives results of approximately 20%, a value that supports previous experiments.

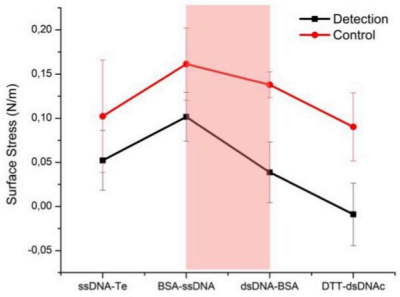

	Measurement (detection)	Positive Values (%)	False Positive (%)
Detection Sample	1	71	0
	2	73	0
	3	26	22
Negative Control Sample	1	0	-
	2	0	-
	3	22	-

Fig. 3. Comparison of surface stress values obtained from two system types (Detection X Control), in the detection step (area highlighted in pale red in the graphic). It was possible to verify that the signal observed was different between the samples. This measurement showed that the presence of immobilized telluride on the microcantilever surface did not interfere in the detection process. It is possible to observe the variation of positive and false positive values between the samples. (For interpretation of the references to colour in this figure legend, the reader is referred to the Web version of this article.)

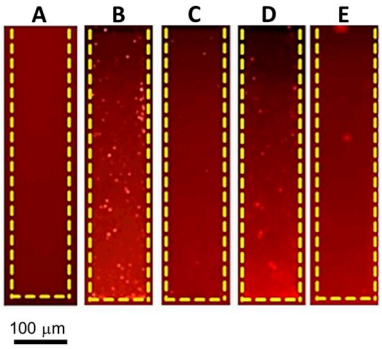

Fig. 4. Images obtained during two DNA immobilization processes: (A) Telluride compound immobilization, (B) first immobilization of T5 DNA-SH-CY3, (C) first reduction of telluride, (D) second immobilization of T5 DNA-SH-CY3 and (E) second reduction of telluride.

3.3. Fluorescence microscopy measurement

The reversible binding property of the organotelluride-functionalized surface, obtained in the previous analyses, fluorescence imaging was performed in oxidation, binding and reduction steps at the microcantilever surface. The microcantilever surface was immobilized with a DNA sequence (T5 DNA-SH-CY3) modified with Cy3 fluorophore. Fig. 4 shows the images obtained in two immobilization cycles.

The images obtained by fluorescence microscopy showed the interaction process of telluride and the thiolate DNA on the surface of the microcantilever. It can be seen that there is not a continuous DNA self-assembled monolayer on the microcantilever surface in the first and second DNA immobilizations, but the interaction between chalcogen and the thiol group present on the DNA structure is not compromised. According to Ndieyira et al. (2008) during the study of detection of antibiotic-mucopeptide binding, the full coverage of the microcantilever surface it is not necessary to obtain a measurable signal, due to the fact that chemically modified regions can connect to each other resulting in a modification of surface stress (Ndieyira et al., 2008). Some studies discuss the behavior of DNA when immobilized on the surface. P. M. Kosaka et al., 2013) presented the self-assembled monolayer of DNA on gold surfaces and observed the formation of DNA islands through Atomic Force Microscopy; reinforcing the present fluorescence microscopy results.

The interaction between telluride and thiol groups was observed only in nuclear magnetic resonance spectrometry (Engman et al., 1992), and the view of this interaction with fluorescence microscopy is innovative, with the application in nanomechanical biosensors.

4. Conclusion

In this work, we demonstrated the viability of organotelluride as a redox agent in reversible immobilizations of thiolate DNA for the detection of complementary DNA probes using nanomechanical systems. The reversibility property allows the reuse of microcantilevers in another modification process, consequently, a new detection. These interactions between organotellurium and thiol groups have been previously observed only in studies about protease inhibition using hypervalent tellurium and selenium derivatives. The results of our study demonstrate an innovative use for the formation of Te-S binding and redox properties of tellurium compounds in biosensing. Our results open a new venue of application of tellurium derivatives as a “new material” that could be useful in areas of research such as micro- and nanomechanical sensors other than organic synthesis and protease inhibition.

CRediT authorship contribution statement

Roseli H. Sato: Conceptualization, Funding acquisition, Formal analysis, Writing - original draft. **Priscila M. Kosaka:** Conceptualization, Funding acquisition, Writing - original draft, Formal analysis. **Álvaro T. Omori:** Formal analysis. **Edgard A. Ferreira:** Funding acquisition. **Denise F.S. Petri:** Formal analysis. **Óscar Malvar:** Funding acquisition. **Carmen M. Domínguez:** Funding acquisition. **Valerio Pini:** Funding acquisition. **Óscar Ahumada:** Formal analysis. **Javier Tamayo:** Formal analysis. **Montserrat Calleja:** Formal analysis. **Rodrigo L.O.R. Cunha:** Conceptualization, Formal analysis, Writing - original draft. **Pablo A. Fiorito:** Conceptualization, Formal analysis, Writing - original draft.

Acknowledgements

We acknowledge the financial support from the CAPES for granting a postgraduate scholarship, the Multiuser Central Facilities (CEM-UFABC) and the Universidade Federal do ABC, Santo André, Brazil. This work was supported by the Spanish Science Ministry (MINECO) through project TEC2017-89765-R and by the European Union's Horizon 2020 research and innovation program under grant agreement No 731868–VIRUSCAN and European Research Council grant 681275 – LIQUIDMASS- ERC- CoG-2015. P M Kosaka acknowledges funding from the Fundación General CSIC ComFuturo Program. We thank Prof. Dr. Erick Leite Bastos from the Universidade de São Paulo, Brazil, for financially supporting the organics analysis (NMR and MS) and Prof. Dr. Willian Reis de Araujo from Unicamp, Brazil, Dr. Letícia Christina Pires Gonçalves and Dr. Nathana Barbosa Lopes for their help in the analysis.

Appendix A. Supplementary data

Supplementary data to this article can be found online at https://doi.org/10.1016/j.bios.2019.04.028.

References

Abondanza, T.S., Oliveira, C.R., Barbosa, C.M.V., Pereira, F.E.G., Cunha, R.L.O.R., Caires,

A.C.F., Comasseto, J.V., Queiroz, M.L.S., Valadares, M.C., Bincoletto, C., 2008. Food Chem. Toxicol. 46 (7), 2540–2545.
Agarwal, D.K., Prasad, A., Vinchurkar, M., Gandhi, S., Prabhakar, D., Mukherji, S., Rao, V.R., 2018. Appl. Nanosci. 8 (5), 1031–1042.
Ahmad, R., Mahmoudi, T., Ahn, M.S., Hahn, Y.B., 2018. Biosens. Bioelectron. 100, 312–325 2018.
Arntz, Y., Seelig, J.D., Lang, H.P., Zhang, J., Hunziker, P., Ramseyer, J.P., Meyer, E., Hegner, M., Gerbe, C., 2003. Nanotechnology 14 (1), 86–90.
Arlett, J.L., Myers, E.B., Roukes, M.L., 2011. Nat. Nanotechnol. 6 (4), 203–215.
Azzam, R.M.A., Bashara, N.M., 1987. Ellipsometry and Polarized Light. North Holland Publications, Amsterdam.
Bañuls, M.J., González-Pedro, V., Barrios, C.A., Puchades, R., Maquieira, Á., 2010. Biosens. Bioelectron. 25 (6), 1460–1466.
Biswal, S.L., Raorane, D., Chaiken, A., Birecki, H., Majumdar, A., 2006. Anal. Chem. 78 (20), 7104–7109.
Boisen, A., Dohn, S., Keller, S.S., Schmid, S., Tenje, M., 2011. Rep. Prog. Phys. 74 (3), 036101.
Buchapudi, K.R., Huang, X., Yang, X., Ji, H.F., Thundat, T., 2011. Analyst 136 (8), 1539–1556.
Caracelli, I., Veja-Teijido, M., Zukerman-Schpector, J., Cezari, M.H.S., Lopes, J.G.S., Juliano, L., Santos, P.S., Comasseto, J.V., Cunha, R.L.O.R., Tiekink, E.R.T., 2012. J. Mol. Struct. 1013, 11–18.
Calleja, M., Nordström, M., Álvarez, M., Tamayo, J., Lechuga, L.M., Boisen, A., 2005. Ultramicroscopy 105 (1–4), 215–222.
Calleja, M., Kosaka, P.M., San Paulo, Á., Tamayo, J., 2012. Nanoscale 4 (16), 4925–4938.
Chen, X., Pan, Y., Liu, H., Bai, X., Wang, N., Zhang, B., 2016. Biosens. Bioelectron. 79, 353–358.
Clark, A.R., Nair, R., Fronczek, F.R., Junk, T., 2002. Tetrahedron Lett. 43 (8), 1387–1389.
Consortium, E.P., 2012. Nature 489, 57–74.
Cunha, R.L.O.R., Urano, M.E., Chagas, J.R., Almeida, P.C., Bincoletto, C., Tersariol, I.L.S., Comasseto, J.V., 2005. Bioorg. Med. Chem. Lett 15 (3), 755–760.
Cunha, R.L.O.R., Gouveia, I.E., Juliano, L., 2009a. An. Acad. Bras. Cienc. 81 (3), 393–407.
Cunha, R.L.O.R., Gouveia, I.E., Feitosa, G.V.P., Alves, M.F., Bromme, D., Comasseto, J.V., Tersariol, I.L.S., Juliano, L., 2009b. Biol. Chem. 390 (11), 1205–1212.
Daniel-Hoffmann, M., Sredni, B., Nitzan, Y., 2012. J. Antimicrob. Chemother. 67 (9), 2165–2172.
Del Rey, M., Silva, R.A., Meneses, D., Petri, D.F.S., Tamayo, J., Calleja, M., Kosaka, P.M., 2014. Sens. Actuators, B 204, 602–610.
Detty, M.R., Friedman, A.E., Oseroff, A.R., 1994. J. Org. Chem. 59 (26), 8245–8250.
Domínguez, C.M., Kosaka, P.M., Sotillo, A., Mingorance, J., Tamayo, J., Calleja, M., 2015. Anal. Chem. 87 (3), 1494–1498.
Duan, X., Rajan, N.K., Routenberg, D.A., Huskens, J., Reed, M.A., 2013. ACS Nano 7 (5), 4014–4021.
Duffy, J., Padovani, F., Brunetti, G., Noy, P., Certa, U., Hegner, M., 2018. Nanoscale 10 (26), 12797–12804.
Edward, D.P., 1985. Handbook of Optical Constants of Solids. Academic Press, Inc., London.
Engman, L., Stern, D., Pelcman, M., 1994. J. Org. Chem. 59 (8), 1973–1979.
Engman, L., Kanda, T., Gallegos, A., Williams, R., Powis, G., 2000. Anti Cancer Drug Des. 15 (5), 323–330.
Engman, L., Stern, D., Cotgreave, I.A., Andersson, C.M., 1992. J. Am. Chem. Soc. 114 (25), 9737–9743.
Eom, K., Park, H.S., Yoon, D.S., Kwon, T., 2011. Phys. Rep. 503 (4–5), 115–163.
Etayash, H., Jiang, K., Azmi, S., Thundat, T., Kaur, K., 2015. Sci. Rep. 5 13967.
Kanda, T., Engman, L., Cotgreave, I.A., Powis, G., 1999. J. Org. Chem. 64 (22), 8161–8169.
Kartanas, T., Ostanin, V., Challa, P.K., Daly, R., Charmet, J., Knowles, T.P.J., 2017. Anal. Chem. 89 (22), 11929–11936 2017.
Kasas, S., Ruggeri, F.S., Benadiba, C., Maillard, C., Stupar, P., Tournu, H., Dietler, G., Longo, G., 2015. Proc. Natl. Acad. Sci. Unit. States Am. 112 (2), 378–381.
Knoglinger, C., Zich, A., Traxler, L., Poslední, K., Friedl, G., Ruttmann, B., Schorpp, A., Müller, K., Zimmermann, M., Gruber, H.J., 2018. Biosens. Bioelectron. 99, 684–690 2018.
Kosaka, P.M., Tamayo, J., Ruz, J.J., Puertas, S., Polo, E., Grazu, V., de la Fuente, J.M., Calleja, M., 2013. Analyst 138, 863–872.
Kosaka, P.M., Gonzalez, S., Dominguez, C.M., Cebollada, A., San Paulo, A., Calleja, M., Tamayo, J., 2013. Nanoscale 5 (16), 7425–7432.
Kosaka, P.M., Pini, V., Ruz, J.J., da Silva, R.A., González, M.U., Ramos, D., Calleja, M., Tamayo, J., 2014. Nat. Nanotechnol. 9 (12), 1047–1053.
Kosaka, P.M., Pini, V., Calleja, M., Tamayo, J., 2017. PLoS One 12 (2), e0171899.
Lan, S., Veiseh, M., Zhang, M., 2005. Biosens. Bioelectron. 20 (9), 1607–1708.
Lee, J.H., Hwang, K.S., Park, J., Yoon, K.H., Yoon, D.S., Kim, T.S., 2005. Biosens. Bioelectron. 20 (10), 2157–2162.
Li, J., He, G., Wang, B., Shi, L., Gao, T., Li, G., 2018. Anal. Chim. Acta 1026, 140–146.
Longo, G., Alonso-Sarduy, L., Rio, L.M., Bizzini, A., Trampuz, A., Notz, J., Dietler, G., Kasas, S., 2013. Nat. Nanotechnol. 8 (7), 522–526.
Loo, L., Wu, W., Shih, W.Y., Shih, W., Borghaei, H., Pourrezaei, K., Adams, G.P., 2011. Sensors 11 (5), 5520–5528.
Malekzad, H., Zangabad, P.S., Mohammadi, H., Sadroddini, M., Jafari, Z., Mahlooji, N., Abbaspour, S., Gholami, S., Ghanbarpoor, M., Pashazadeh, R., Beyzavi, A., Karimi, M., Hamblin, M.R., 2018. TrAC Trends Anal. Chem. (Reference Ed.) 100, 116–135.
Maluf, S.E.C., Melo, P.M.S., Varotti, F.P., Gazarini, M.L., Cunha, R.L.O.R., Carmona, A.K., 2016. Parasitol. Int. 65 (1), 20–22.
Malvar, O., Ruz, J.J., Kosaka, P.M., Domínguez, C.M., Gil-Santos, E., Calleja, M., Tamayo, J., 2016. Nat. Commun. 7, 13452 2016.
Mertens, J., Rogero, C., Calleja, M., Ramos, D., Martín-Gago, J.A., Briones, C., Tamayo, J., 2008. Nat. Nanotechnol. 3 (5), 301–307.
Ndieyira, J.W., Watari, M., Barrera, A.D., Zhou, D., Vogtli, M., Batchelor, M., Cooper, M.A., Strunz, T., Horton, M.A., Abell, C., Rayment, T., Aeppli, G., McKendry, R.A., 2008. Nat. Nanotechnol. 3 (11), 691–696.
Nogueira, C.W., Zeni, G., Rocha, J.B.T., 2004. Chem. Rev. 104 (12), 6255–6285.
Pandya, H.J., Roy, R., Chen, W., Chekmareva, M.A., Foran, D.J., Desai, J.P., 2015. Biosens. Bioelectron. 63, 414–424.
Persike, D.S., Cunha, R.L.O.R., Juliano, L., Silva, I.R., Rosim, F.E., Vignoli, T., Dona, F., Cavalheiro, E.A., Fernandes, M.J.S., 2008. Neurobiol. Dis. 31 (1), 120–126.
Pimentel, I.A.S., Paladi, C.S., Katz, S., Judice, W.A.S., Cunha, R.L.O.R., Barbieri, C.L., 2012. PLoS One 7 (11), e48780 2012.
Ramos, D., Mertens, J., Calleja, M., Tamayo, J., 2007. Sensors 7 (9), 1757–1765.
Silberman, A., Kalechman, Y., Hirsch, S., Erlich, Z., Sredni, B., Albeck, A., 2016. Chembiochem 17 (10), 918–927.
Tanini, D., Grechi, A., Ricci, L., Dei, S., Teodori, E., Capperucci, A., 2018. New J. Chem. 42 (8), 6077–6083.
Viter, R., Tereshchenko, A., Smyntyna, V., Starodub, N., Yakimova, R., Khranovskyy, V., Ramanavicius, A., 2017. Sensor. Actuator. B Chem. 252, 95–102.
Wang, J., Morton, M.J., Elliott, C.T., Karoonuthaisiri, N., Segatori, L., Biswal, S.L., 2014. Anal. Chem. 86 (3), 1671–1678.
Wu, G., Datar, R.H., Hansen, K.M., Thundat, T., Cote, R.J., Majumdar, A., 2001. Nat. Biotechnol. 19 (9), 856–860.
You, Y., Ahsan, K., Detty, M.R., 2003. J. Am. Chem. Soc. 125 (16), 4918–4927.
Zhou, L., Fang, S., Liu, Y., Yang, R., Song, D., Long, F., Zhu, A., 2018. Chemosphere 210, 10–18.
Zhou, M.H., Meng, W.L., Zhang, C.Y., Li, X.B., Wua, J.Z., Zhang, N.H., 2018. Soft Matter 14, 3028–3039 2018.